Mineralogical Magazine (2019), **83**, 223–231
doi:10.1180/mgm.2018.88

CAMBRIDGE UNIVERSITY PRESS

Article

The new mineral novograblenovite, $(NH_4,K)MgCl_3{\cdot}6H_2O$ from the Tolbachik volcano, Kamchatka, Russia: mineral description and crystal structure

Viktor M. Okrugin[1], Sharapat S. Kudaeva[1], Oxana V. Karimova[2]*, Olga V. Yakubovich[2,3], Dmitry I. Belakovskiy[4], Nikita V. Chukanov[5], Andrey A. Zolotarev[6], Vladislav V. Gurzhiy[6], Nina G. Zinovieva[3], Andrey A. Shiryaev[2,7] and Pavel M. Kartashov[2]

[1]Institute of Volcanology and Seismology FEB RAS, Piip Boulevard 9, Petropavlovsk-Kamchatsky, 683006, Russia; [2]Institute of Geology of Ore Deposits, Geochemistry, Mineralogy and Petrography (IGEM) RAS, Staromonetny 35, 119017 Moscow, Russia; [3]Faculty of Geology, Moscow State University, Vorobievy Gory, 119899 Moscow, Russia; [4]Fersman Mineralogical Museum RAS, Leninskiy Prospect, 18/2, 119071 Moscow, Russia; [5]Institute of Problems of Chemical Physics, Russian Academy of Sciences, Chernogolovka, Moscow region, 142432 Russia; [6]Institute of Earth Sciences, Saint-Petersburg State University, University Emb. 7/9, 199034 Saint-Petersburg, Russia; and [7]Frumkin Institute of Physical Chemistry and Electrochemistry RAS, Leninsky prospect, 31, korp. 4, 119071 Moscow, Russia

Abstract

The new mineral novograblenovite, $(NH_4,K)MgCl_3{\cdot}6H_2O$, was found on basaltic lava from the 2012–2013 Tolbachik fissure eruption at the Plosky Tolbachik volcano, Kamchatka Peninsula, Russia. It occurs as prismatic, needle-like transparent crystals together with gypsum and halite. Novograblenovite was formed due to the exposure of the host rocks to eruptive gas exhalations enriched in HCl and NH_3. Basalt was the source of potassium and magnesium for the mineral formation. Novograblenovite crystallises in the monoclinic space group $C2/c$, with unit-cell parameters $a = 9.2734(3)$ Å, $b = 9.5176(3)$ Å, $c = 13.2439(4)$ Å, $\beta = 90.187(2)°$, $V = 1168.91(2)$ Å^3 and $Z = 4$. The five strongest reflections in the powder X-ray diffraction pattern [d_{obs}, Å (I, %) (h k l)] are: 3.330 (100) (2 2 0), 2.976 (45) ($\bar{1}$ 1 4), 2.353 (29) ($\bar{2}$ 2 4), 3.825 (26) (2 0 2), 1.997 (25) ($\overline{4}$ 2 2). The density calculated from the empirical formula and the X-ray data is 1.504 g cm^{-3}. The mineral is biaxial (+) with $\alpha = 1.469(2)$, $\beta = 1.479(2)$ and $\gamma = 1.496(2)$ ($\lambda = 589$ nm); $2V_{meas.} = 80(10)°$ and $2V_{calc.} = 75.7°$. The crystal structure (solved and refined using single-crystal X-ray diffraction data, $R_1 = 0.0423$) is based on the perovskite-like network of $(NH_4,K)Cl_6$-octahedra sharing chlorine vertices, and comprises $[Mg(H_2O)_6]^{2+}$ groups in framework channels. The positions of all independent H atoms were obtained by difference-Fourier techniques and refined isotropically. All oxygen, nitrogen and chlorine atoms are involved in the system of hydrogen bonding, acting as donors or acceptors. The formula resulting from the structure refinement is $[(NH_4)_{0.7}K_{0.3}]MgCl_3{\cdot}6H_2O$. The mineral is named after Prokopiy Trifonovich Novograblenov, one of the researchers of Kamchatka Peninsula, a teacher, naturalist, geographer and geologist.

Keywords: novograblenovite, new mineral, ammonium potassium magnesium chloride hydrate, crystal structure, Plosky Tolbachik volcano, Kamchatka.

(Received 1 February 2018; accepted 18 April 2018)

Introduction

The present paper describes the mineralogical and crystal chemical description of the new species novograblenovite, $(NH_4,K)MgCl_3{\cdot}6H_2O$, based on its chemical composition, crystal structure and physical properties. It also contains a discussion on topological and genetic interconnections of the new mineral and related natural and synthetic phases.

Novograblenovite is named after Prokopiy Trifonovich Novograblenov (August 14, 1892–January 1, 1934), a researcher of Kamchatka Peninsula, a teacher, naturalist, geographer and geologist. He published papers on botany, geology, zoology and archaeology. The most important of Novograblenov's works are "*Catalogue of Kamchatka Volcanoes*" (Novograblenov 1932) and "*Hot Springs of Kamchatka*" (Novograblenov 1931). P.T. Novograblenov perished due to political repressions in 1934.

The new mineral and its name have been approved by the IMA Commission on New Minerals, Nomenclature and Classification (IMA2017-060, Okrugin *et al.*, 2017). The cotype specimen is deposited in the systematic collection of the Fersman Mineralogical Museum, Russian Academy of Sciences, Moscow, Russia, with the registration number 5003/1.

Occurrence, morphology and physical properties

The mineral novograblenovite was discovered on the basaltic lava of the 2012–2013 Tolbachik fissure eruption at the southern slope of the Plosky Tolbachik volcano, Kamchatka Peninsula,

*Author for correspondence: Oxana V. Karimova, Email: oxana.karimova@gmail.com
Associate Editor: G. Diego Gatta
Cite this article: Okrugin V.M., Kudaeva S.S., Karimova O.V., Yakubovich O.V., Belakovskiy D.I., Chukanov N.V., Zolotarev A.A., Gurzhiy V.V., Zinovieva N.G., Shiryaev A.A. and Kartashov P.M. (2019) The new mineral novograblenovite, $(NH_4,K)MgCl_3{\cdot}6H_2O$ from the Tolbachik volcano, Kamchatka, Russia: mineral description and crystal structure. *Mineralogical Magazine* **83**, 223–231. https://doi.org/10.1180/mgm.2018.88

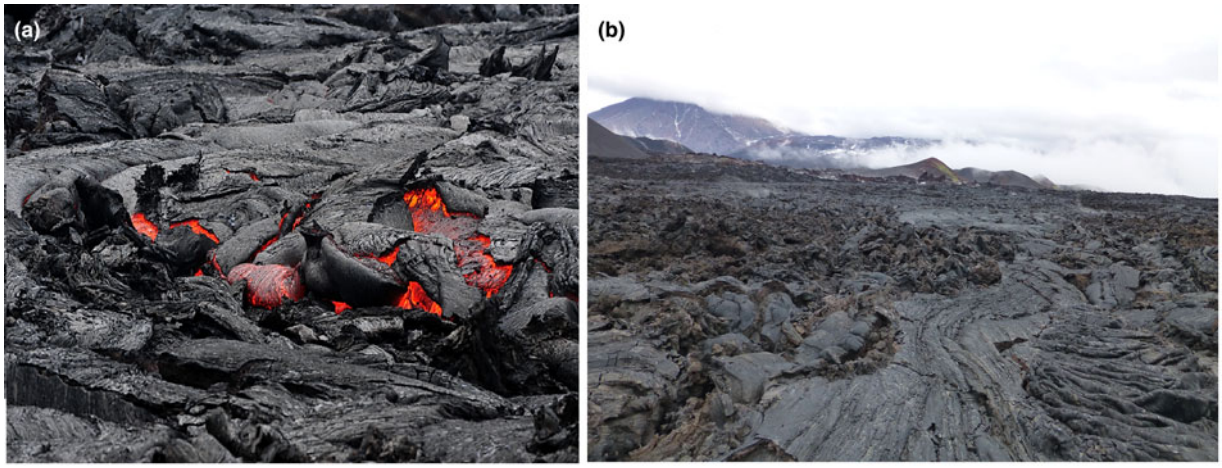

Fig. 1. Plosky Tolbachik volcano eruption: the black basaltic lava flows in June 2013 (*a*) and in October 2013 (*b*).

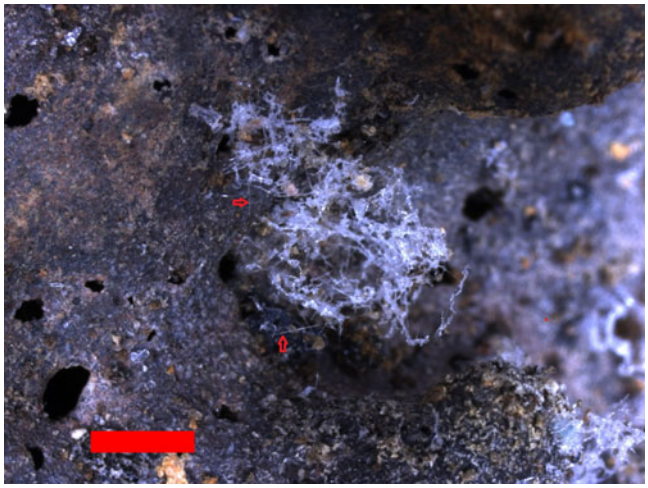

Fig. 2. Fibrous aggregate of novograblenovite crystals on basalt. Scale bar = 1000 μm.

Far-Eastern Region, Russia (55°45′28.8″N, 160°18′39.3″E). Here, novograblenovite occurs in association with gypsum and halite.

Plosky Tolbachik is spatially and genetically connected with two radial linear zones of slag cones (Tolbchinsky Dol – a broad lava plain with an area of ~875 km^2), extending in the submeridional direction on either side of it at distances up to 20 km to the north-east and ~50 km to the south. Plosky (= flat) Tolbachik volcano has the form of a truncated cone, its top is cut by a Hawaiian-type caldera of 3 km diameter (Okrugin, 2013). It is one of two volcanoes in the Tolbachik volcano complex.

The mineral samples were collected from black basaltic lava that had a thick (5–10 mm) hardened vitreous crust and columnar parting (Fig. 1). The surface of these lava flows is characterised by a peculiar needle-like glassy texture. The basaltic lava under the crust has a porous texture with cavities up to 10 mm across. Long-prismatic, needle-like transparent crystals of the new mineral were found within these cavities together with gypsum and halite. Novograblenovite was formed due to exposure of the host rock to eruptive gas exhalations enriched in HCl and NH_3. Basalt was the source of potassium and magnesium for the mineral formation.

The mineral forms isolated transparent, colourless, imperfect acicular crystals up to 1 mm (typically, 0.2–0.5 mm) long and open-work fibrous aggregates up to 2 mm across (Figs 2, 3). It is characterised by a white streak and vitreous lustre, and is non-fluorescent. Novograblenovite is brittle; thin fibres are flexible. Its Mohs hardness is 1–2. Cleavage or parting is not observed and the fracture is even. The density could not be measured directly because of the small size of individual crystals and the open-work character of aggregates. Calculations from the empirical formula and the X-ray data gives 1.504 g cm^{-3}. Novograblenovite is soluble in water, alcohol and acetone; it dissolves in hydrochloric acid without gas evolution.

The mineral is biaxial (+) with $\alpha = 1.469(2)$, $\beta = 1.479(2)$ and $\gamma = 1.496(2)$ ($\lambda = 589$ nm); $2V_{meas.} = 80(10)°$ and $2V_{calc.} = 75.7°$.

Dispersion of the optical axes $r > v$ is very weak. In the sections parallel to the optical axes plane $c \wedge Z = 40°$. In transmitted light the mineral is colourless and non-pleochroic.

Infrared spectroscopy

An infrared (IR) spectrum of novograblenovite (Fig. 4) was obtained using a SpectrumOne FTIR spectrometer coupled with an AutoImage microscope with a spectral resolution of 1 or 2 cm^{-1}; 256 scans were collected. The sample was placed on a gold mirror, and the spectrum obtained is a superposition of transmission and reflectance signals with strong predominance of the former. Rectangular apertures matching crystal dimensions (i.e. 50 × 150 or 30 × 150 μm) were employed; several different spots were analysed from every crystal to assure consistency of the results.

For comparison, an ATR spectrum of natural carnallite from the RRUFF database (entry R050353 http://rruff.info/)/R050353) and an IR spectrum of synthetic $NH_4MgCl_3{\cdot}6H_2O$ (Wheeler and Wypyski, 1993) are also shown (Fig. 4). The spectrum of novograblenovite is close to that of the synthetic NH_4-carnallite analogue (Wheeler and Wypyski, 1993). In the spectrum of the novograblenovite specimen studied a strong feature at 1409 with a shoulder at 1420 cm^{-1} characterises bending modes of ammonium ions (ν_4); superposition of broad bands in the range from 2200 to 3200 cm^{-1} is due to stretching modes of NH_4^+ ions. A sharp peak at 1655 cm^{-1} probably corresponds to the ν_2 mode of NH_4Cl. The broad band in the interval 2800–3800 cm^{-1} matches O–H and N–H valence vibrations. The relatively narrow peak at 3553 cm^{-1} might be related to a bridging hydroxyl. The

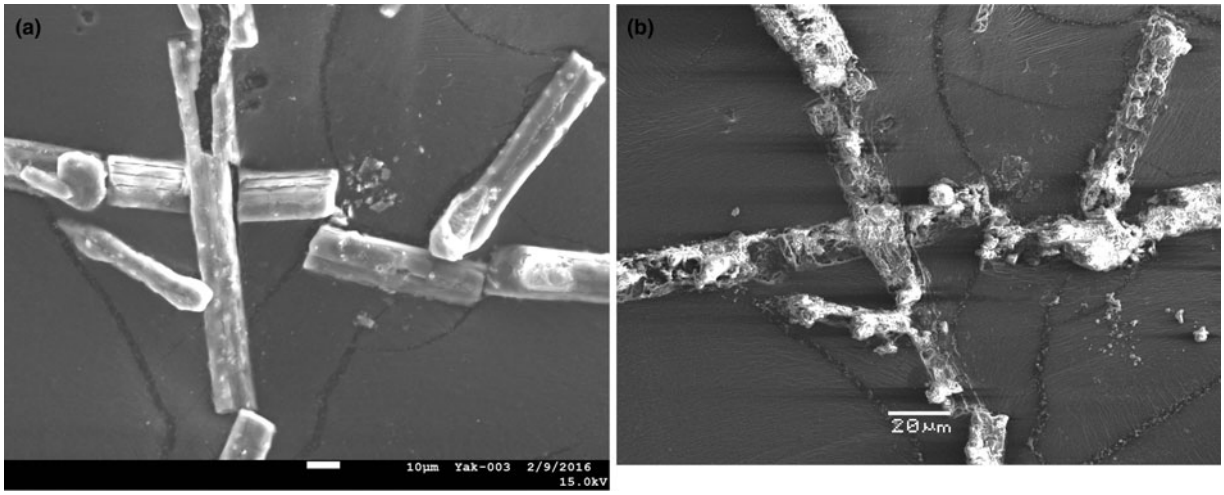

Fig. 3. Novograblenovite crystals: (*a*) in February 2016, scale bar = 10 µm; (*b*) in June 2016, scale bar = 20 µm. Scanning electron microscopy (secondary electron) images; specimen number 5003/1.

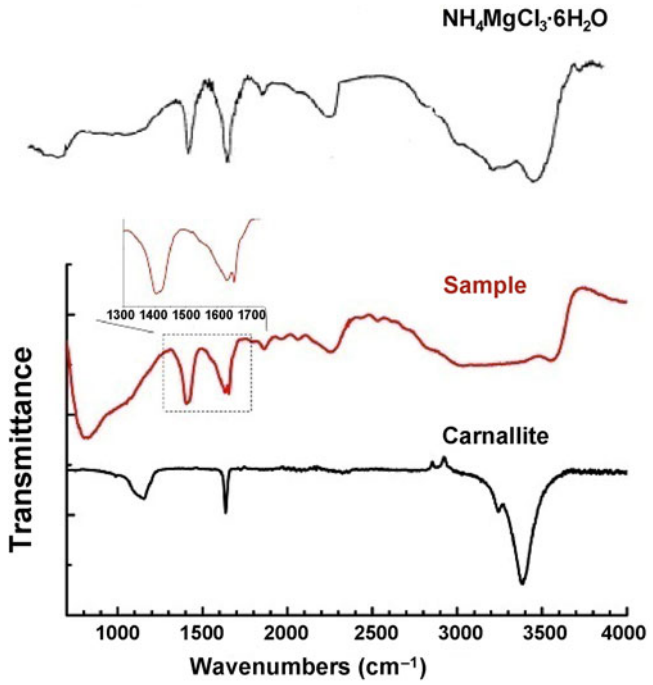

Fig. 4. Infrared spectra of novograblenovite ('sample'), natural carnallite (RRUFF R050353) and synthetic compound $NH_4MgCl_3{\cdot}6H_2O$ (from Wheeler and Wypyski, 1993).

band at 1630 cm^{-1} and the absorption above 3200 cm^{-1} are due to O–H vibrations. A peak at 2256 cm^{-1} and weak bands in the range 1800–2200 cm^{-1} most probably characterise combination bands. An absence of the 2256 cm^{-1} peak in the pure carnallite spectrum suggests ammonia ion librations (broad band at ~800 cm^{-1}) contributed to this band in our case.

Chemical data

The chemical composition of cotype material was acquired using a Jeol JSM-6480LV scanning electron microscope equipped with an Oxford X-Max^N energy-dispersive spectrometer (EDS) (Laboratory of Analytical Techniques of High Spatial Resolution, Department of Petrology, Geological Faculty, Moscow State University). Samples of novograblenovite were carbon coated and analysed using the following conditions: 10 kV acceleration voltage; 1.4 nA beam current; and analysed area 14 µm^2. The data acquisition rate was 10,000–12,000 counts/s, with 20–25% dead time and 25 s live time. Under these conditions the dispersion of measured concentrations of main elements did not exceeded 0.5 relative%, and detection limits were 0.05–0.1 wt.% for all elements analysed. Element concentrations were measured using the *K*α lines for N, O, K, Mg and Cl. The standards employed were: microcline (K), Al_2O_3 (O), MgO (Mg), NaCl (Na and Cl), and internal standard BN for N. The presence of N was also evident in the EDS spectrum (Fig. 5). X-ray intensities were converted to wt.% by the XPP quantitative analysis software of Oxford Instruments (UK). This analytical method was chosen because the sample would be severely damaged by using the wavelength dispersive spectroscopy technique, even with a low voltage and a large diameter beam. The mineral is destroyed by polishing techniques and damaged under the electron beam (Fig. 3). Therefore, the analysis of the chemical composition of novograblenovite was performed on an unpolished surface; 17 areas (14 µm^2), near to planar, were chosen for the scanning electron analyses. The mean analytical results are reported in Table 1 and Fig. 6. The chemical formulae obtained from the chemical analysis and the crystal structure are: $[(NH_4)_{0.70}K_{0.45}]_{1.15}Mg_{1.00}Cl_{2.55}{\cdot}6H_{1.92}O_{0.96}$ and $[(NH_4)_{0.70}K_{0.30}]_{1.00}MgCl_3{\cdot}6H_2O$, respectively. The difference in the formulae and the scatter of the sums of the novograblenovite analyses are related to the fact that the EDS experiment was carried out on an unpolished surface; and also that the mineral is destroyed under the electron beam. The lowered O content, as well as the lowered content of calculated H may be due to partial dehydration of the mineral (see Fig. 3*b*). The H_2O content was calculated based on the structure refinement (see below). The presence of H_2O is also confirmed by the IR spectrum.

The simplified formula is $(NH_4,K)MgCl_3{\cdot}6H_2O$. The end-member formula is $(NH_4)MgCl_3{\cdot}6H_2O$, which requires N 5.46, Mg 9.47, Cl 41.41, O 37.38, H 6.28, total 100.00 wt.%.

The Gladstone-Dale compatibility index (Mandarino, 1981) calculated from the empirical formula and unit-cell parameters

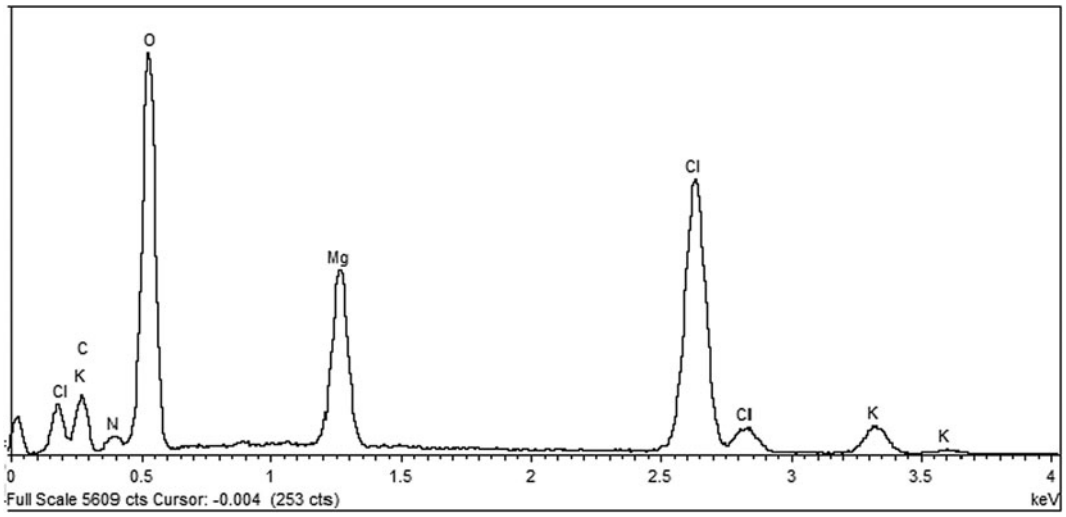

Fig. 5. Energy-dispersive spectrum for novograblenovite.

Table 1. Composition (in wt.%) of novograblenovite.

	Data from EDS						Calculated from the structure	
	Elements				Oxides			
Constituent	Wt.%*	S.D.	Range	Pfu	Constituent	Wt.%	Wt.% of elements	Pfu
N	3.8	1.0	2.3–6.2	0.70	$(NH_4)_2O$**	7.0	3.7	0.70
O	35.2	4.1	26.5–41.2	5.77	H_2O**	28.8	36.5	6.00
Mg	9.3	0.8	8.2–10.5	1.00	MgO	15.4	9.2	1.00
Cl	34.5	1.2	33.1–36.2	2.55	Cl	34.5	40.4	3.00
K	6.7	0.8	5.1–8.0	0.45	K_2O	8.1	4.6	0.30
H**	5.5						5.6	
Total	89.5	5.8	76.5–98.2	10.48		93.8	100.0	11.00
Total***	95.0							

*The mean analytical results of 17 analyses; **calculated from the structure; ***includes additional H calculated from the structure.
S.D. – standard deviation. Pfu – per formula unit.

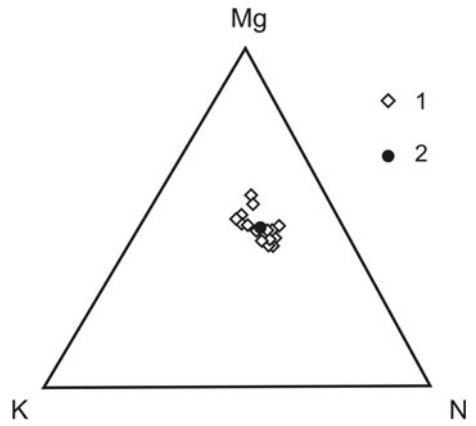

Fig. 6. Diagram of EDS-analyses (at.%) made on 17 relatively planar areas (14 μm^2) of unpolished crystals of novograblenovite (1) and their mean composition (2).

determined from powder X-ray diffraction data is $1 - (K_P/K_C) = -0.058$ (good).

X-ray crystallography

Powder X-ray diffraction data (Table 2) were obtained using a Rigaku R-AXIS Rapid II diffractometer equipped with a cylindrical image plate detector, with Debye-Scherrer geometry (diameter = 127.4 mm; Co*K*α radiation). The data were integrated using the software package *OSC2XRD* (Britvin *et al.*, 2017). The indexing of the powder-diffraction pattern was made by comparison with the pattern calculated after the crystal-structure determination. The powder data show good agreement with those calculated from the structure refinement. Parameters of the monoclinic unit cell refined from the powder data are: a = 9.2734(3) Å, b = 9.5176(3) Å, c = 13.2439(4) Å, β = 90.187(2)° and V = 1168.91(2) Å^3. No twinning of the crystals is apparent. The most common forms are: {100} and {010}.

X-ray diffraction intensities of reflections were collected for the best tested sample on a Bruker DUO CCD single-crystal diffractometer equipped with a micro-focus X-ray tube (Mo*K*α radiation). Data collection included a total of 10,084 reflections. The intensities were integrated and corrected for Lorenz and polarisation effects, for background, and for beam decay using the Bruker *SAINT* program. A semi-empirical absorption correction was applied on the basis of intensities of equivalent reflections using the Bruker *SADABS* program, however, it was found to be negligible.

All calculations were performed with *SHELX* programs (Sheldrick, 2015*a*,*b*) in the framework of a *WinGX* software package (Farrugia, 2012). The crystal structure was solved *via* direct methods in the space group *C*2/*c* and refined against the

Table 2. Observed and calculated powder X-ray diffraction data (d in Å) for novograblenovite*.

I_{obs}	I_{calc}	d_{obs}	d_{calc}	$h\ k\ l$
13	7, 3	6.66	6.642, 6.624	110, 002
14	9, 10	4.701	4.695, 4.685	$\bar{1}12$, 112
22	39	3.883	3.865	022
26	28, 27	3.825	3.804, 3.793	202, $\bar{2}02$
100	100, 49	3.330	3.321, 3.312	220, 004
16	3	3.191	3.237	023
45	30, 17	2.976	2.966, 2.940	$\bar{1}14$, 222
14	6 , 4	2.875	2.872, 2.868	$\bar{3}\bar{1}1$, 311
14	7, 2	2.731	2.733, 2.718	132, 024
11	5, 7, 4	2.689	2.699, 2.691, 2.684	$\bar{2}04$, 202, 312
11	18	2.391	2.379	400
29	24, 25, 3	2.353	2.348, 2.343, 2.342	$\bar{2}24$, 224, 041
18	4, 4, 9	2.254	2.239, 2.225, 2.223	042, $\bar{1}34$, 134
1	3, 4	2.202	2.202, 2.186	$\bar{3}\bar{1}4$, 402
14	3, 5, 5	2.106	2.117, 2.101, 2.094	240, $\bar{3}\bar{3}2$, 116
17	21, 12	2.024	2.017, 2.003	$\bar{2}\bar{4}2$, 026
25	16, 21, 7	1.997	1.991, 1.999, 1.987	206, $\bar{4}\bar{2}2$, 422
10	10	1.942	1.932	044
11	9, 9	1.907	1.9018, 1.897	$\bar{4}04$, 404
4	8, 4	1.666	1.660, 1.656	440, 008
3	9	1.507	1.501	262
7	11, 11	1.490	1.483, 1.483	$\bar{2}23$, 440
3	5, 7	1.365	1.367, 1.359	265, 043
2	7, 8	1.347	1.345, 1,342	$\bar{6}\bar{2}2$, 622
3	3, 2, 2	1.292	1.288, 1.285, 1.284	068, $\bar{4}\bar{6}2$, 462
2	2, 2, 2	1.277	1.276, 1.273, 1.271	0.2.10, $\bar{6}42$, 642
1	1	1.219	1.223	510
2	3, 3	1.178	1.174, 1.171	$\bar{4}40$, 446
1	3, 1, 3	1.128	1.125, 1.122, 1.120	4.6.10, $\bar{2}42$, 246

*The strongest lines are given in bold.

Table 3. Crystal information and details of X-ray data collection and refinement.

Crystal data	
Ideal formula	$[(NH_4)_{0.7}K_{0.3}]Mg(H_2O)_6Cl_3$
Crystal dimensions (mm)	0.20 × 0.04 × 0.03
Crystal system, space group	Monoclinic, $C2/c$
Temperature (K)	296(2)
a, b, c (Å)	9.250(6), 9.499(6), 13.228(8)
β (°)	90.152(15)
V (Å^3)	1162.3(13)
Z	4
Absorption μ (mm^{-1})	0.941
$D_{calc.}$ (g cm^{-3})	1.504
Data collection	
Crystal description	White needle
Diffractometer	Bruker Goniometer; DUO detector
Radiation type, wavelength (Å)	Mo$K\alpha$ (0.71073)
Scanning mode	ω scan, δφ = 0.5°
θ range (°)	max θ = 28.883°
Absorption correction	Multi-scan (SADABS, Bruker Analytical X-ray Systems)
T_{min}, T_{max}	0.789, 0.991
No. of measured, independent and observed [I >2σ(I)] reflections	10,084, 1512, 1074
R_σ	0.038
$R_{int.}$	0.054
Indices range of h, k, l	$-12 \le h \le 12$, $-12 \le k \le 11$, $-17 \le l \le 17$
Refinement	
No. of refined parameters	80
Residuals R (observed reflections)	0.0423
R, wR_2 (all reflections)	0.0620, 0.1234
Goodness of fit, S	1.069
$\Delta\rho_{max}$, $\Delta\rho_{min}$ (e^- Å^{-3})	0.483 /−0.274

Table 4. Atom coordinates and equivalent isotropic displacement parameters.

Atom	x/a	y/b	z/c	U_{eq} (Å^2)*
Cl1	½	½	½	0.0449(3)
Cl2	0.75210(6)	0.73751(6)	0.74695(4)	0.0442(2)
Mg1	0	½	½	0.0246(2)
$M1$	½	0.4985(2)	¾	0.0531(9)
O1	0.1806(2)	0.6015(2)	0.44890(14)	0.0451(4)
O2	0.4090(2)	0.1875(2)	0.53789(14)	0.0442(4)
O3	0.9102(2)	0.5139(2)	0.35973(13)	0.0448(5)
H1	0.438(3)	0.262(3)	0.523(2)	0.060(9)
H2	0.875(3)	0.447(3)	0.334(2)	0.055(8)
H3	0.876(3)	0.581(3)	0.339(2)	0.062(9)
H4	0.261(4)	0.572(4)	0.467(2)	0.073(10)
H5	0.187(3)	0.641(4)	0.402(2)	0.065(10)
H6	0.352(3)	0.204(3)	0.585(3)	0.073(10)
H7	0.433	0.551	0.755	0.17(3)
H8	0.494	0.460	0.710	0.17(3)

*Isotropic displacement parameters for hydrogen atoms. Occupancy factors for $M1$: 0.302(8) K + 0.698(8) N; H7: 0.70; H8: 0.70.

F^2 data to the final R factor of 0.0423 (for 1074 unique reflections with $I > 2\sigma(I)$) with anisotropic displacement parameters for non-hydrogen atoms. A refinement of the occupancies of the N sites revealed significant substitution of the ammonium ions for K^+. The eight independent positions of H atoms were obtained by difference-Fourier techniques and most of them were refined in an isotropic approximation. The coordinates of H7 and H8 atoms forming ammonium groups were fixed in the last run of refinement in order to maintain a reasonable geometry of the NH_4^+ ion and N–H···Cl hydrogen bonds. The formula resulting from the structure refinement $[(NH_4)_{0.70}K_{0.30}]MgCl_3{\cdot}6H_2O$ (for $Z = 4$) reasonably coincides to that obtained by scanning electron microanalysis (taking into account that an unpolished sample was used).

The crystallographic characteristics, the experimental parameters of data collection and structure refinement are summarised in Table 3. The final results for the atom positions are presented in Table 4, while Table 5 reports characteristic distances and angles. The crystallographic information files have been deposited with the Principal Editor of *Mineralogical Magazine* and are available as Supplementary material (see below).

Crystal structure description

The main units forming the novograblenovite structure are shown in Fig. 7. These are Mg^{2+} cations in an octahedral environment of H_2O molecules and NH_4^+/K^+ ions at the centre of octahedra built by Cl atoms. Note, that $(NH_4)^+$ and K^+ ions are distributed statistically in one position in a ratio of ~2:1. In nearly regular MgO_6 octahedra, the Mg–O distances vary from 2.034(2) to 2.045(2) Å. The (NH_4,K)–Cl distances range from 3.257(2) to 3.375(2) Å (Table 5).

Large $(NH_4,K)Cl_6$-octahedra share chlorine vertices to form a three-dimensional framework topologically identical to that built from TiO_6 octahedra in perovskite. The perovskite-type network is stabilised by $[Mg(H_2O)_6]^{2+}$ cations, which occupy positions in framework channels parallel to [001] and [110] directions (Fig. 8), and are connected with $(NH_4,K)Cl_6$-polyhedra through the system of O–H···Cl asymmetric hydrogen bonds formed by water molecules and chlorine atoms (Table 6). Obviously, the N–H···Cl hydrogen bonds act in ~⅔ cases in accordance with the statistical occupancy of the MCl_6 ($M = NH_4$ or K) octahedra by the ammonium ions. Each chlorine atom accepts six hydrogen

Table 5. Selected interatomic distances (Å) and angles (°).

Mg octahedron		K octahedron		∠H–O–H in H_2O molecules		∠H–N–H in NH_4 tetrahedron	
Mg1–O2	2.033(2) ×2	K1–Cl2	3.255(2) ×2	H4–O1–H5	110(3)	H7–N1–H7′	103(3)
Mg1–O3	2.035(2) ×2	K1–Cl1	3.307(2) ×2	H1–O2–H6	104(3)	H8–N1–H8′	111(3)
Mg1–O1	2.045(2) ×2	K1–Cl2′	3.377(2) ×2	H2–O3–H3	111(3)	H7–N1–H8	111(3)
<Mg–O>	2.041	<K–Cl>	3.320			H7′–N1–H8′	111(3)

Symmetry code for H7′ and H8′: 1 – *x*, *y*, 1.5 – *z*; for Cl2′: *x* – 0.5, *y* – 0.5, *z*.

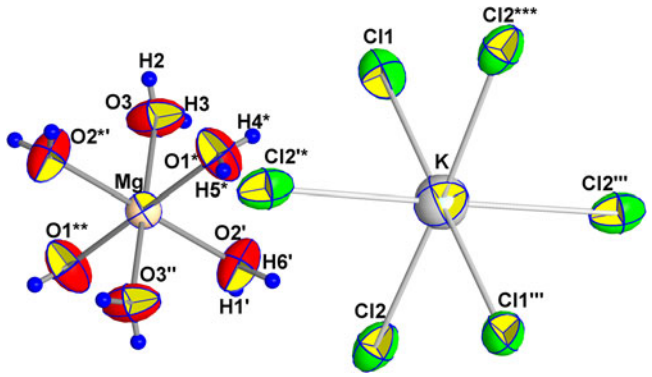

Fig. 7. Novograblenovite. Basic structural units with atom labelling scheme. Displacement ellipsoids at the 70% probability level. [Symmetry codes (*) 1 – *x*, 1 – *y*, 1 – *z*; (**) 1 + *x*, *y*, *z*; (***) –½ + *x*, –½ + *y*, *z*; (') ½ + *x*, ½ + *y*, *z*; ('') 2 – *x*, 1 – *y*, 1 – *z*; (''') 1 – *x*, *y*, 1½ – *z*; (*') 1½ – *x*, ½ – *y*, 1– *z*; (**') 1½ – *x*, –½ + *y*, ½ – *z*].

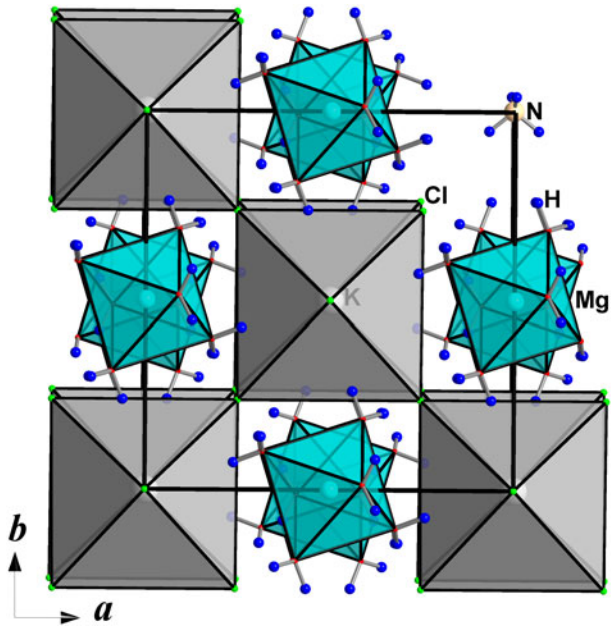

Fig. 8. The crystal structure of the novograblenovite in *xy* projection.

bonds: four from O atoms at the vertices of $Mg(H_2O)_6$ octahedra and two from the ammonium ions. The O–H····Cl hydrogen bonds lie in the interval 3.127(3)–3.178(3) Å, while N–H····Cl bonds are normally longer and vary from 3.255(2) to 3.375(2) Å (Table 6). The N–H7····Cl2 distance of 3.255(2) Å is somewhat shorter compared to the expected value of ~3.3 Å. This bond shortening is evidently due to the mixed N/K occupancy of the corresponding site in the structure. An even shorter N/K–Cl distance of 3.220(2) Å has been reported in the crystal structure

Table 6. Geometric characteristics of hydrogen bonds*.

D–H···*A* (Å)	*d*(*D*–H) (Å)	*d*(H···*A*) (Å)	∠*DHA* (°)	*d*(*D*···*A*) (Å)
O2–H1···Cl1	0.78(3)	2.36(3)	171(3)	3.127(3)
O3–H2···Cl2	0.79(3)	2.38(3)	173(3)	3.171(2)
O3–H3···Cl2	0.76(3)	2.38(3)	169(3)	3.132(2)
O1–H4···Cl1	0.82(4)	2.36(4)	173(3)	3.179(3)
O1–H5···Cl2	0.73(3)	2.43(3)	170(3)	3.150(2)
O2–H6···Cl2	0.83(4)	2.36(4)	163(3)	3.162(2)
N1–H7···Cl2	0.80(4)	2.46(4)	171(4)	3.255(2)
N1–H8···Cl1	0.65(4)	2.80(4)	137(4)	3.307(2)

*D – donor of hydrogen bond, *A* – hydrogen bond acceptor.

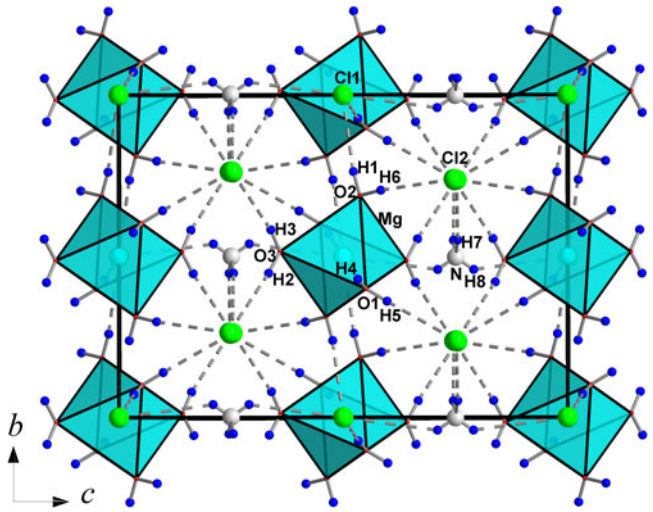

Fig. 9. The scheme of hydrogen bonding in the crystal structure of novograblenovite.

of adranosite-(Fe) (Mitolo *et al.*, 2013). Thus, all oxygen, nitrogen and chlorine atoms in the crystal structure are involved in the system of hydrogen bonding, acting as donors or acceptors. Hydrogen bonding in this structure serves as an important mechanism providing linkage between the main structural fragments (Fig. 9).

A bond-valence calculation has been performed using the algorithm and parameters given by Pyatenko (1972) (Table 7). Valence contributions of the H atoms in the O–H····Cl hydrogen bonds were estimated from the H–Cl distances using the algorithm of Brown and Altermatt (1985), and bond-valence parameters (R_o and *b*) suggested by Malcherek and Schlüter (2007). Data from Table 7 clearly confirm the assignment of H_2O ligands.

Crystal chemical and genetic relationships with formula analogues

Novograblenovite has a natural formula analogue, the mineral carnallite, $KMgCl_3{\cdot}6H_2O$. Despite similar chemical compositions

Table 7. Bond-valence data for novograblenovite*.

Atom	Mg1	*M*1**	H1	H2	H3	H4	H5	H6	Σ
O1	0.329×2↓					0.885	0.844		2.06
O2	0.335×2↓		0.861					0.866	2.06
O3	0.335×2↓			0.889	0.838				2.06
Cl1		0.168×2↓×2→	0.139×2→			0.115×2→			0.84
Cl2		0.173×2↓		0.111	0.162		0.156	0.134	0.89
		0.158×2↓							
Σ	2.00	1.00	1.00	1.00	1.00	1.00	1.00	1.00	

*Multiplicity is indicated by 2↓ and 2→. **$M1$: $K_{0.30}(NH_4)_{0.70}$.

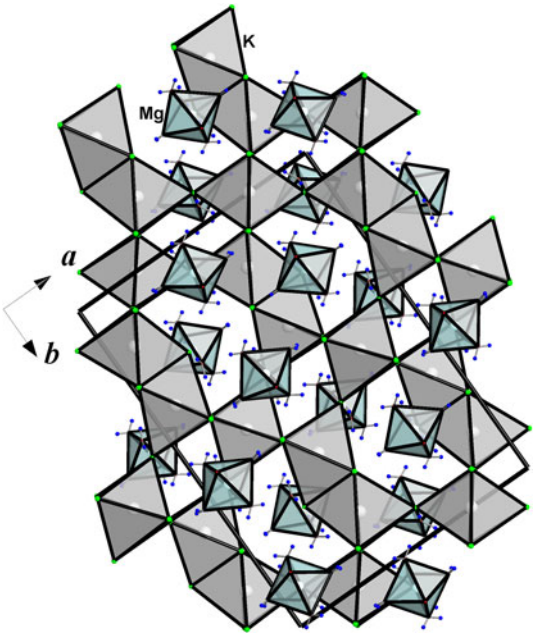

Fig. 10. The carnallite, $KMg(H_2O)_6Cl_3$ crystal structure in *xy* projection.

these mineral species are characterised by diverse crystal structures (Fischer, 1973; Schlemper *et al.*, 1985). The perovskite, $CaTiO_3$-type, structure of novograblenovite where large Ca atoms are replaced by the $Mg(H_2O)_6$ complexes affects the comparison with carnallite significantly. In the novograblenovite structure there is exclusively corner linkage between $(NH_4,K)Cl_6$ octahedra, however in carnallite ⅔ of the KCl_6 octahedra share faces (Schlemper *et al.*, 1985) (Fig. 10). A similar interconnection of TiO_6 octahedra sharing faces occurs in a hexagonal $BaTiO_3$-type structure (Fischer, 1973; Schlemper *et al.*, 1985). Carnallite is thought to crystallise in saline marine deposits by reaction of pre-existing saline minerals with fluids high in potash, while novograblenovite has an effusive origin; it forms under exposure to eruptive gas exhalations enriched in HCl and NH_3, and by extracting potassium and magnesium from the basaltic lava. This is similar to the conditions of adranosite formation in the La Fossa crater, Sicily – rather high activities of free ammonia and volatile chlorides in the gas prevent the dissociation of novograblenovite, ensuring its stability (Demartin *et al.*, 2010). Thus, the distinct conditions of development of the formula analogues of carnallite and novograblenovite may initiate their structural dissimilarity.

Several synthetic phases in the framework of $AMg(H_2O)_6Cl_3$ composition ($A = NH_4$, Rb or Cs) obtained in the course of fractional crystallisation and slow evaporation from a solution, have been studied (Solans *et al.*, 1983; Waizumi *et al.*, 1991*a*,*b*; Marsh, 1992*a*,*b*). All three varieties exhibit the same monoclinic perovskite-like crystal structure as established for novograblenovite (Table 8).

Generally, the mineral carnallite (Schlemper *et al.*, 1985) and its synthetic analogue $KMg(H_2O)_6Cl_3$ (Fischer, 1973)

Table 8. Pseudocubic minerals and synthetic compounds related to novograblenovite.

Mineral name/formula	Unit-cell param. (Å)	Angles (β, °)	Space group, *Z*	*V* (Å^3)	ρ (g/cm^3)	<Mg–O> (Å)	Crystal morphology	Reference
$NH_4MgCl_3{\cdot}6H_2O$	*a* = 9.320(3) *b* = 9.582(3) *c* = 13.327(4)	90.12(4)	*C*2/*c*, 4	1190(1)	1.43	2.053	Equi-dimensional	Solans *et al.* (1983)
Novograblenovite $[(NH_4,K)MgCl_3{\cdot}6H_2O]$	*a* = 9.250(6) *b* = 9.499(6) *c* = 13.228(8)	90.152(15)	*C*2/*c*, 4	1162(3)	1.50	2.038	Needles	This work
Carnallite $[KMgCl_3{\cdot}6H_2O]$	*a* = 16.119(3) *b* = 9.551(2) *c* = 22.472(4)		*Pncn*, 12	3460(1)	1.60	2.045	Prismatic crystals	Schlemper *et al.* (1985)
$RbMgCl_3{\cdot}6H_2O$	*a* = 9.270 *b* = 9.553 *c* = 13.282(4)	90.17	*C*2/*c*, 4	1176	1.83	2.043	Equi-dimensional	Marsh (1992*a*,*b*)
$CsMgCl_3{\cdot}6H_2O$*	*a* = 9.450 *b* = 9.642 *c* = 13.495(2)	90.19	*C*2/*c*, 4	1230	2.00	–	Equi-dimensional	Waizumi *et al.* (1991*b*)
$LiMgCl_3{\cdot}7H_2O$	*a* = 9.2322(3) *c* = 12.0541(5)		*R*3, 3	889.8(1)	1.48	2.055	Equi-dimensional	Schmidt *et al.* (2009)

*Converted from the originally reported triclinic unit cell in view of the transformation made by Marsh (1992*a*,*b*) for the Rb analogue.

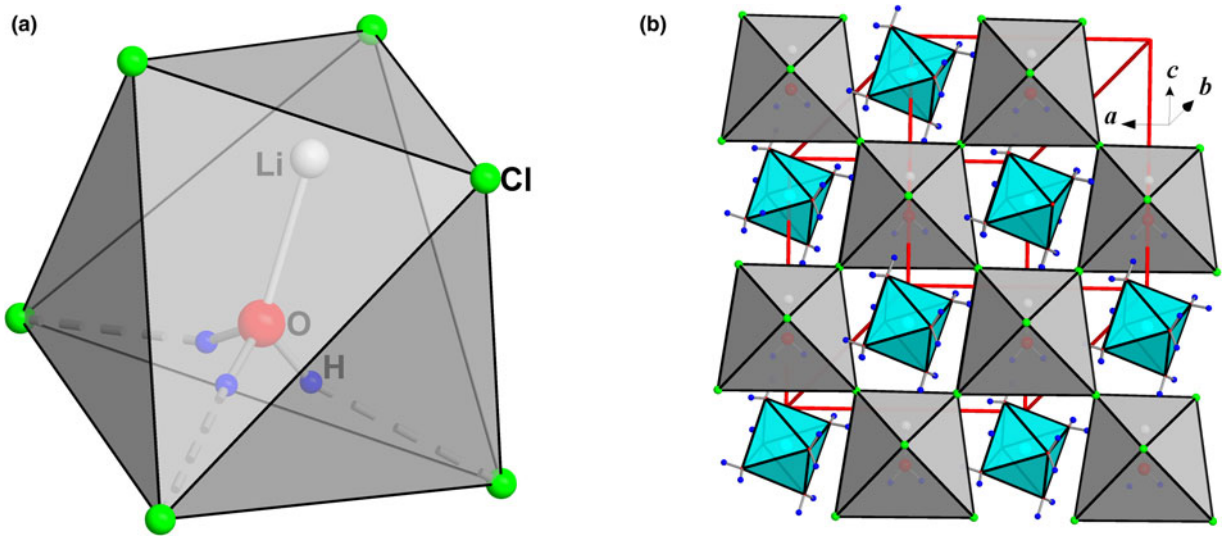

Fig. 11. 'Li carnallite': the $[Li(H_2O)]^+$ unit in an octahedral surrounding of Cl atoms (only two H atoms of the water molecule are distributed equally over three energetically equivalent positions) (*a*) and a three-dimensional network stabilised by $Mg(H_2O)_6$ octahedra (*b*).

demonstrate alternate orthorhombic structures as discussed above. In agreement with the observation made in Wizumi *et al.* (1991*b*), the size of ionic radius, being somewhat smaller for K^+ compared to NH_4^+, Rb^+ and Cs^+, plays a crucial role here, and hence may be responsible for a change of structure type. The synthetic compound $LiMg(H_2O)_7Cl_3$ is also close in composition and shows a trigonal crystal structure based on a network of $Mg(H_2O)_6$ octahedra and $Li(H_2O)Cl_3$ tetrahedra connected *via* O–H····Cl hydrogen bonds (Schmidt *et al.*, 2009). In order to simulate a perovskite-like network of MCl_6 octahedra, the small alkaline Li adopts the water molecule at 1.890 Å to form $[Li(H_2O)]^+$ cation complexes. The $[Li(H_2O)]^+$ unit as a coordination centre is surrounded by Cl anions to form five-vertex polyhedra $Li(H_2O)Cl_4$ with three Li–Cl bonds of 2.3806(10) Å and two H····Cl bonds of 2.53(5) Å (Fig. 11*a*). The $Li(H_2O)Cl_4$ polyhedra share chlorine vertices with a three-dimensional network as shown in Fig. 11*b*. As in the previously described alkaline hydrate chlorides, the crystal structure is stabilised by $Mg(H_2O)_6$ octahedra, which are connected to Cl atoms *via* O–H····Cl hydrogen bonds.

Acknowledgements. We thank an anonymous member of the IMA-CNMNC who informed us that nograblenovite is likely to be very close to "redikortsevite", described without IMA approval as fumarole product from a burning mine dump in the Chelyabinsk coal basin, Russia (Chesnokov, *et al.*, 1988), also found later in Germany (Witzke, 1996) and Poland (Stachowicz, *et al.*, 2011). We also acknowledge partial support of M. V. Lomonosov Moscow State University Program of Development. The XRD experiments were carried out using the facilities of XRD Resource Centres of St. Petersburg University. We are much obliged to the Editors, Stuart Mills and Peter Leverett, for handling the manuscript and for useful suggestions.

Supplementary material. To view supplementary material for this article, please visit https://doi.org/10.1180/mgm.2018.88.

References

Britvin S.N., Dolivo-Dobrovolsky D.V. and Krzhizhanovskaya M.G. (2017) Software for processing of X-ray powder diffraction data obtained from the curved image plate detector of Rigaku RAXIS Rapid II diffractometer. *Zapiski RMO* (*Proceedings of the Russian Mineralogical Society*), **146**, 104–107 [in Russian].

Brown I.D. and Altermatt D. (1985) Bond valence parameters obtained from a systematic analysis of the inorganic crystal structure database. *Acta Crystallographica*, **B41**, 244–247.

Chesnokov B.V., Bazhenova L.F., Shcherbakova E.P., Michal T.A. and Deriabina T.N. (1988) New minerals from the burned dumps of the Chelyabinsk coal basin. Pp. 5–31 in: *Mineralogy, Technogenesis, and Mineral-Resource Complexes of the Urals*. Special Issue, Ural Branch of the Academy of Sciences SSSR [in Russian].

Demartin F., Gramaccioli C.M. and Campostrini I. (2010) Adranosite, $(NH_4)_4NaAl_2(SO_4)_4Cl(OH)_2$, a new ammonium sulfate chloride from La Fossa crater, vulcano, Aeolian islands, Italy. *The Canadian Mineralogist*, **48**, 315–321.

Farrugia L.J. (2012) WinGX and ORTEP for Windows: an update. *Journal of Applied Crystallography*, **45**, 849–854.

Fischer W. (1973) Die Kristalstruktur des Carnallits KMgCl3.6H2O. *Neues Jahrbuch für Mineralogie – Monatshefte*, 100–109 [in German].

Malcherek Th. and Schlüter J. (2007) $Cu_3MgCl_2(OH)_6$ and the bond-valence parameters of the OH—Cl bond. *Acta Crystallographica*, **B63**, 157–160.

Mandarino J.A. (1981) The Gladston-Dale relationship: Part IV. The compatibility concept and its application. *The Canadian Mineralogist*, **19**, 441–450.

Marsh R.E. (1992*a*) Structure of $MgCl_2.RbCl.6H_2O$. Corrigendum. *Acta Crystallographica*, **C48**, 218–219.

Marsh R.E. (1992*b*) Structure of $MgCl_2.RbCl.6H_2O$: amplification and apology. *Acta Crystallographica*, **C48**, 972.

Mitolo D., Demartin F., Garavelli A., Campostrini I., Pinto D., Gramaccioli C.M., Acquafredda P. and Kolitsch U. (2013) Adranosite-(Fe), $(NH_4)_4NaFe_2(SO_4)_4Cl(OH)_2$, a new ammonium sulfate chloride from La Fossa crater, vulcano, Aeolian islands, Italy. *The Canadian Mineralogist*, **51**, 57–66.

Novograblenov P.T. (1931) Hot Springs of Kamchatka. *News State geographical society*, **63**, 500–505.

Novograblenov P.T. (1932) Catalogue of Kamchatka volcanoes. *News State geographical society*, **64**, 88–99.

Okrugin V.M. (2013) Volcanic fantasy, the third month. *Mining Bulletin of Kamchatka*, **23**, 79–92 [in Russian].

Okrugin V.M., Kudaeva S.S., Karimova O.V., Yakubovich O.V., Belakovskiy D.I., Chukanov N.V., Zolotarev A.A., Gurzhiy V.V., Zinovieva N.G., Shiryaev A.A. and Kartashov P.M. (2017) Novograblenovite, IMA 2017-060. CNMNC Newsletter No. 39, October 2017, page 1284; *Mineralogical Magazine*, **81**, 1279–1286.

Pyatenko Yu.A. (1972). Unified approach to analysis of local balance of valences in inorganic structures. *Soviet Physics, Crystallography*, **17**, 677–682.

Schlemper E.O., Sen Gupta P.K. and Zoltai T. (1985) Refinement of the structure of carnallite, $Mg(H_2O)_6KCl_3$. *American Mineralogist*, **70**, l309–1313.

Schmidt H., Euler B, Voigta W. and Heide G. (2009) Lithium carnallite, $LiCl.MgCl_2.7H_2O$, *Acta Crystallographica*, **C65**, i57–i59.

Sheldrick G.M. (2015*a*) *SHELXT* – Integrated space-group and crystal structure determination. *Acta Crystallographica*, **A71**, 3–8.

Sheldrick G.M. (2015*b*) Crystal structure refinement with *SHELXL*. *Acta Crystallographica*, **C71**, 3–8.

Solans X., Font-Altaba D.M., Aguiló M., Solans J. and Domenech V. (1983) Crystal form and structure of ammonium hexaaquamagnesium trichloride, $NH_4[Mg(H_2O)_6]Cl_3$. *Acta Crystallographica*, **C39**, 1488–1490.

Stachowicz M., Parafiniuk J., Baginski B., Macdonald R. and Wozniak K. (2011): Structural analysis of new mineral phases. *Acta Crystallographica*, **A67**, C573 [abstract].

Waizumi K., Masuda H., Ohtaki H., Burkov K.A. and Scripkin M.Y. (1991*a*) Structure of $MgCl_2.RbCl.6H_2O$. *Acta Crystallographica*, **C47**, 251–254.

Waizumi K., Masuda H., Ohtaki H., Scripkin M.Y. and Burkov K.A. (1991*b*) Crystallographic investigations of $[Mg(H_2O)_6]XCl_3$ double salts ($X^+ = K^+$, Rb^+, Cs^+, NH_4^+): Crystal structure of $[Mg(H_2O)_6]X$Cl3. *American Mineralogist*, **76**, 1884–1888.

Wheeler G.S. and Wypyski M.T. (1993) An unusual efflorescence on Greek ceramics. *Studies in Conservation*, **38**, 55–62.

Witzke T. (1996) Die Minerale der brennenden Halde der Steinkohlengrube "Deutschlandschacht" in Oelsnitz bei Zwickau. *Aufschluss*, **47**, 41–48 [in German].